Multistep Dissociation of Fluorine Molecules under Extreme Compression

Defang Duan,[1] Zhengtao Liu,[1] Ziyue Lin,[1] Hao Song,[1] Hui Xie,[1] Tian Cui,[2,1,*]
Chris J. Pickard,[3,4] and Maosheng Miao[5,6,*]
[1]*State Key Laboratory of Superhard Materials, College of Physics, Jilin University, Changchun 130012, China*
[2]*Institute of High Pressure Physics, School of Physical Science and Technology, Ningbo University, Ningbo 315211, China*
[3]*Department of Materials Science & Metallurgy, University of Cambridge,*
27 Charles Babbage Road, Cambridge CB3 0FS, United Kingdom
[4]*Advanced Institute for Materials Research, Tohoku University, 2-1-1 Katahira, Aoba, Sendai 980-8577, Japan*
[5]*Department of Chemistry and Biochemistry, California State University, Northridge, California 91220, USA*
[6]*Department of Earth Science, University of California Santa Barbara, California 93106, USA*

(Received 10 December 2020; revised 31 March 2021; accepted 29 April 2021; published 4 June 2021; corrected 24 August 2021)

All elements that form diatomic molecules, such as H_2, N_2, O_2, Cl_2, Br_2, and I_2, are destined to become atomic solids under sufficiently high pressure. However, as revealed by many experimental and theoretical studies, these elements show very different propensity and transition paths due to the balance of reduced volume, lone pair electrons, and interatomic bonds. The study of F under pressure can illuminate this intricate behavior since F, owing to its unique position on the periodic table, can be compared with H, with N and O, and also with other halogens. Nevertheless, F remains the only element whose solid structure evolution under pressure has not been thoroughly studied. Using a large-scale crystal structure search method based on first principles calculations, we find that, before reaching an atomic phase, F solid transforms first into a structure consisting of F_2 molecules and F polymer chains and then into a structure consisting of F polymer chains and F atoms, a distinctive evolution with pressure that has not been seen in any other elements. Both intermediate structures are found to be metallic and become superconducting, a result that adds F to the elemental superconductors.

DOI: 10.1103/PhysRevLett.126.225704

Many elements, such as H, N, O, and Cl, form diatomic molecules under ambient conditions. At high enough pressure they are destined to transform into atomic phases, accompanied by emerging properties such as metallization and high T_c superconductivity. Being the most abundant element, hydrogen, although containing only one electron in its shell, is very resistant to molecular dissociation and undergoes a series of structure changes before eventually transforming into atomic phases under extremely high pressures (>550 GPa) [1]. Intermediate phases show complex structural features, such as the coexistence of two types of H. Computational predictions [2,3] and experimental evidence [4] reveal that the corresponding phase contains alternating layers formed by two different types of H_2 molecules.

The dissociation of elementary molecules and transformation into atomic phases is dictated by the number of valence electrons. More electrons delay the formation of atomic phases. B and C are stable as covalent solids under ambient pressures, whereas N, due to its peculiar electron counting, forms the exceedingly strong $N \equiv N$ triple bonds and the most stable diatomic molecule. However, despite the presence of many metastable phases, its stable molecular phase evolves directly into an atomic "cubic gauche" phase at a modest pressure of about 110 GPa [5,6]. Its atomic phases show intricate structural variations, such as the predicted N_{10} diamondoid structure at 263 GPa [7] and an all-nitrogen metallic salt at 2.5 TPa [8], respectively. Compared to N, O has six valence electrons, a number that is suitable for a double $O = O$ bond and two lone electron pairs on each O. Although O_2 molecules consist of weaker bonds than N_2, counterintuitively, they are much more resistant to dissociation and persist up to 1.9 TPa, beyond which they form polymeric spiral chain and zigzag chain structures [9,10]. The next element is fluorine, in which the diatomic bond is weaker than in both N_2 and O_2 since the number of its valence electrons permits the formation only of single bonds. Nevertheless, no study, theoretical or experimental, has demonstrated the dissociation of F_2 under pressure. The x-ray powder diffraction studies of Meyer *et al.* indicated that α-F_2 is monoclinic with two candidate space groups $C2/m$ and $C2/c$ of solid fluorine at ambient pressure [11]. Lv *et al.* performed an *ab initio* calculation and found that the $C2/m$ structure is dynamically unstable, and that the $C2/c$ structure transforms to $Cmca$ above 8 GPa and remains stable up to 100 GPa [12].

The behavior of F_2 molecules under pressure can also be compared with diatomic molecules of other halogens such as Cl_2, Br_2, and I_2. The metallization and dissociation of these molecules have been observed experimentally. Solid molecular I_2 becomes a mixed-molecular structure at 12.5 GPa [13], and an insulator to metal transition occurs at about 16 GPa, keeping molecular characteristic, and dissociates into an incommensurate modulated structure at about 23 GPa [14]. The incommensurate structure transforms to an atomic phase with space group $Immm$ at 30 GPa, then to $I4/mmm$ at 45 GPa, and finally to the Fm-$3m$ phase at 53 GPa [15]. The Cl_2 and Br_2 solids share a common phase transition with I_2, but the transition pressures are higher [16,17]. Recent experiments show that the mixed-molecular structure, metallization, and molecular dissociation for Cl_2 occurs at about 130, 200, and 258 GPa, respectively [18]. Remarkably, both I and Br are found to become superconducting with $T_c = 1.2$ and 1.5 K at 28 and 90 GPa, respectively [19], which is consistent with theoretical predictions [20,21]. Together with those for metallic hydrogen, these results suggest that superconductivity might be a ubiquitous phenomenon, accompanying molecular dissociation under pressure.

In this Letter, we report on an unexpected and unique structural evolution of F_2 molecular crystal under high pressure, obtained from extensive structure searches in conjunction with first principles calculations. Strikingly, instead of transforming directly from molecular phases to atomic or extended phases like H, N, and O, fluorine undergoes transitions into two intermediate structures, one that is stable from 2.8 to 4 TPa consists of both F_2 molecules and polymeric F chains, and another that is stable from 4 to 30 TPa consists of both F atoms and polymeric F chains. The true atomic phase of F can be obtained only under extremely high pressures beyond 30 TPa, clearly revealing the distinct resistance of F toward the transition to an atomic phase. Despite the remaining molecular features in the intermediate structures, they are found to be superconducting, albeit with low T_c of only a few kelvins.

A structure prediction is the key to a computational materials discovery [22]. We searched for low enthalpy structures of fluorine in the multiterapascal range using the *ab initio* random structure searching (AIRSS) method [23,24]. This approach has been applied to many systems, including hydrogen [2,3], oxygen [10], and nitrogen [8], at high pressures. AIRSS based structure predictions were performed at selected pressures of 0.5, 1, 2, 3, 4, 5, 10, 20, 30, and 40 TPa and on different cell sizes containing up to 30 atoms. The validity of the potentials and the exchange correlation functionals have also been tested, the results are shown in Figs. S1–S3 of the Supplemental Material [25]. Details of these computational methods and parameters are provided in the Supplemental Material [25].

Figure 1 shows the pressure dependence of enthalpy for structures that are found in this Letter as well as the most stable structures from previous studies. Strikingly, the molecular $Cmca$ phase that was found to be stable from 8 to 100 GPa persists up to 2.75 TPa. The low-pressure molecular phases such as $C2/m$ and $C2/c$ are omitted because they are stable only below 8 GPa and their enthalpies are very close to that of $Cmca$. At 2.75 TPa, F transforms from the $Cmca$ structure to a $P6/mcc$ structure and then, at 4 GPa, to a $Pm\bar{3}n$ structure. This structure is surprisingly stable in a large pressure range and transforms to an $Fddd$ structure only at 30 TPa. As shown by the calculated phonon spectra (Fig. S4 of the Supplemental Material [25]), no structure shows dynamic instability in the pressure ranges that are predicted to be thermodynamically stable.

Apart from the exceedingly wide range of stable pressures, the structures of these phases show a striking feature—namely, the coexistence of atomic, molecular, and polymeric F atoms in the same structure. Although similar abnormal structural features were reported in amorphous N_2 [32] and SO_2 [33] recently, it remains a surprise that all three different stages of structural evolution of the light p-block elements can coexist in thermodynamically stable crystalline phases. Among the four stable structures, $Cmca$ is a pure molecular phase and $Fddd$ is a true atomic phase. The nearest F-F distances in $Cmca$ at 1 TPa are calculated to be 1.28 Å, while the next nearest F-F distances are 1.55 Å, which clearly shows the F_2 molecular character in this structure. For comparison, the bond length of F_2 molecules in the gas phase is 1.43 Å. With increasing pressure, both the nearest and next nearest F-F distances decrease but the molecular features remain throughout its stable pressure range.

In contrast to the $Cmca$ and $Fddd$ structures, there are two types of F atoms in the two intermediate structures, F^1 and F^2 in $P6/mcc$ and F^2 and F^0 in $Pm\bar{3}n$. The F^1/F^2 and F^2/F^0 ratios are 6:1 and 3:1 in these two structures, respectively. As shown in Fig. 2, $P6/mcc$ consists of layers of F_2 molecules formed by F^1 atoms; whereas F^2 atoms form straight polymeric chains that are perpendicular to the F_2 molecule planes. At 3 TPa, the nearest F^1-F^1 distance is 1.17 Å, and the next nearest F^1-F^1 distance is 1.41 Å and is inside the F_2 planes. In contrast, the nearest F^2-F^2 distance in the chain is 1.32 Å, indicating a weaker bond with F^1-F^1. The neighboring F^1-F^2 distance is 1.56 Å, which is significantly larger than the neighboring distances between F atoms of the same type. Interestingly, the structural motifs of F_2 planes are very similar to several high pressure structures of H_2 [2], such as the $P6_3/m$ and $C2/c$ structures. In particular, the topology of the F_2 planes in the $P6/mcc$ structure is identical to that of the H_2 planes in the $P6_3/m$ structure [see Fig. 2(b)]. The major difference is that the vertical H atoms form H_2 molecules in $P6_3/m$, whereas the vertical F^2 atoms in $P6/mcc$ form linear chains, as shown in Fig. 2(a).

Although both the $P6/mcc$ and $Pm\bar{3}n$ structures consist of two types of F atoms, the structural features of the two are distinctly different. Interestingly, $Pm\bar{3}n$ is identical to

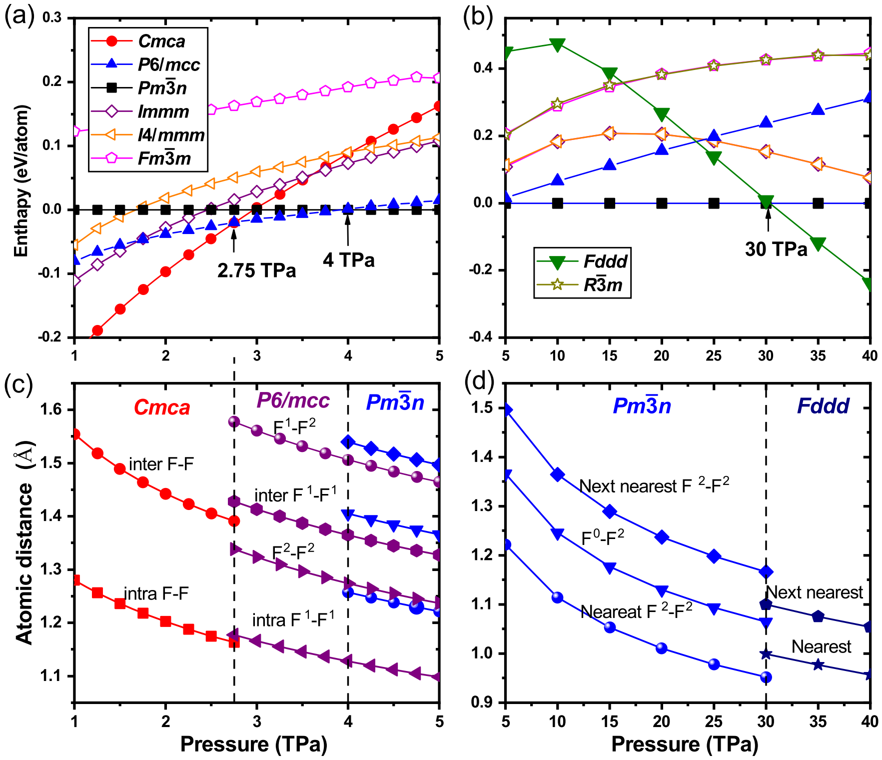

FIG. 1. (a),(b) Enthalpies of various structures relative to the $Pm\bar{3}n$ structure as functions of pressure. (c),(d) Interatomic distances as a function of pressure, including the nearest F-F distances (intra F-F) and the next nearest F-F distances (inter F-F) in the $Cmca$ phase; the nearest F^1-F^1 distance (intra F^1-F^1), the next nearest F^1-F^1 distance (inter F^1-F^1), the nearest F^2-F^2 distance, and the neighboring F^1-F^2 distance in the $P6/mcc$ phase; the nearest F^2-F^2 distance, the neighboring F^0-F^2 distance, the next nearest F^2-F^2 distance in the $Pm\bar{3}n$ phase; and the nearest and next nearest F-F distance in the $Fddd$ phase.

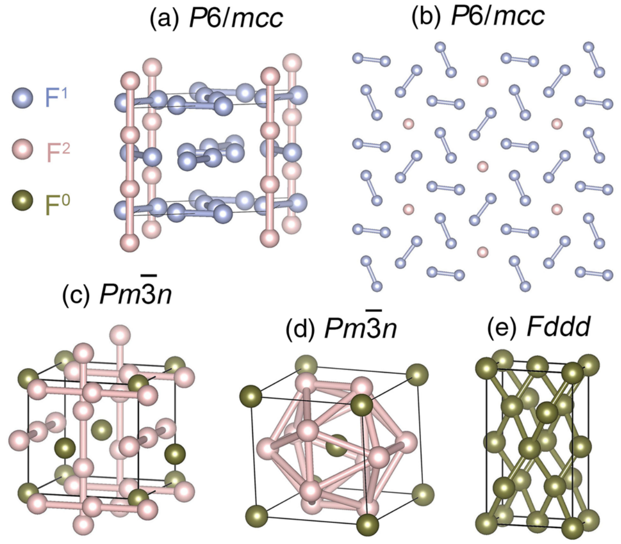

FIG. 2. (a) Crystal structure and (b) layer of $P6/mcc$. The F^1, F^2, and F^0 are shown using blue, pink, and dark yellow spheres, respectively. The layers are stacked in an $ABXBA$ fashion. The crystal structure of $Pm\bar{3}n$ showing (c) polymeric line chains and (d) icosahedron. (e) Crystal structure of $Fddd$.

$A15$ structures of some binary compounds, such as Cr_3Si, except that F plays the roles of both constituents in $A15$. The major difference versus the $P6/mmc$ structure is that there are no F_2 molecules in this structure. This does not mean that F has transformed into an atomic phase, because, as in all $A15$ structures, the F^2 atoms form polymeric chains, with different bonding features than the F^0 atoms. Correspondingly, at 5 TPa, the nearest F^2-F^2 distance in $Pm\bar{3}n$ structure is 1.22 Å, which is slightly smaller than the F^2-F^2 distance of 1.24 Å in $P6/mcc$ line chains. Each F^0 atom has 12 neighboring F^2 atoms, with F^0-F^2 distance of 1.37 Å at 5 TPa. The F^2 atoms surrounding the F^0 atom can be viewed as forming a deformed icosahedron. The distance of one edge of the distorted icosahedron is 1.22 Å (the nearest F^2-F^2), and the other edge distance is 1.50 Å (the next nearest F^2-F^2). Such cage structures are common in compounds formed by group 14 elements (C, Si, Ge) at ambient condition but rarely seen in solids under very high pressures. A well-known exception is the N_{10} cage structure in diamondoid nitrogen [7].

The mixed molecular-polymeric F in $P6/mcc$ and mixed polymeric-atomic F in $Pm\bar{3}n$ structures are also revealed distinctively by their bonding nature. Electron localization functions (ELFs) can distinguish the bond type and strength

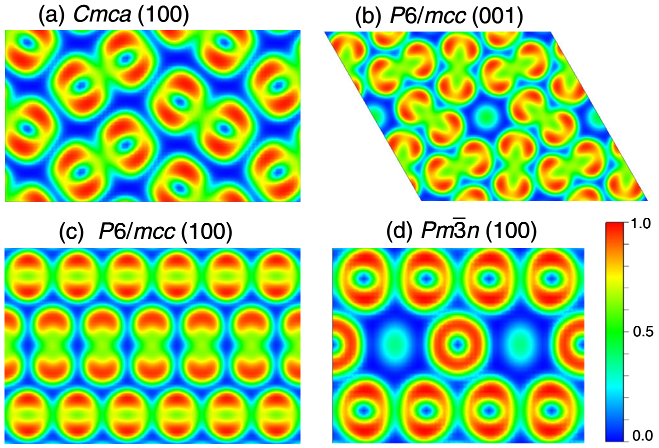

FIG. 3. The calculated ELF of our predicted phases. (a) *Cmca* in the (100) section at 3 TPa. (b),(c) $P6/mcc$ in the (001) and (100) sections at 3 TPa. (d) $Pm\bar{3}n$ in the (100) section at 5 TPa.

and are therefore calculated for the two structures. As shown in Fig. 3, ELFs show not only strong covalent bonds in F_2 molecules in *Cmca* and $P6/mcc$ structures but also considerably stronger bonds between neighboring F^2 atoms in the line chains in $P6/mcc$ and $Pm\bar{3}n$ structures. The F^1 atoms in neighboring molecules in the same F_2 plane are also moderately bonded in the $P6/mcc$ structure. On the other hand, ELF values between the F^1 and F^2 atoms in $P6/mcc$ and the F^0 and F^2 atoms in $Pm\bar{3}n$ are small, indicating weak bonding between them.

The structural evolution of solid F under pressure is accompanied by changes in the electronic structure as shown in Fig. 4. The molecular *Cmca* phase has a significant electronic gap that decreases with pressure up to 500 GPa and then increases with pressure throughout its stable pressure range. At 2.75 TPa, the transition pressure to the $P6/mcc$ phase, its gap becomes 2.65 eV, as calculated by density-functional theory (DFT) using the Perdew-Burke-Ernzerhof functional. The change of the band gap in *Cmca* structure is the result of the two competing effects. Under increasing pressure, it is reduced by the increasing intermolecular interactions, and increased by the contraction of the F—F bonds. In contrast to the molecular phase, the two intermediate phases, $P6/mcc$ and $Pm\bar{3}n$, and the atomic phase, *Fddd*, are all metallic. Interestingly, as shown by the projected density of states (PDOS), the F_2 molecules in $P6/mcc$ contribute significantly to the electron density at the Fermi level, demonstrating that the metallization might happen without regard to the dissociation of the F_2 molecules, similar to H_2 and other halogens. Also, at the Fermi level of the $P6/mcc$ structure, the PDOS of polymeric F (F^2) is very low and the PDOS of the molecular F (F^1) shows a dip, with both leading to poor metallicity. In contrast, $Pm\bar{3}n$ shows a much higher DOS at the Fermi level, with contributions from both the polymeric F (F^2) and the atomic F (F^0). Furthermore, *Fddd*, as an atomic phase, shows a typical band structure of metals and a high DOS at the Fermi level. We also calculated the band structure and the density of sates of $P6/mcc$ using the Heyd-Scuseria-Ernzerhof (HSE06) hybrid functional [34]. Although the results show slight changes—for example, the HSE06 functional opens a small gap at the Γ point—the major features of the electronic structure remain the same (Fig. S5 in the Supplemental Material [25]).

Since the intermediate $P6/mcc$ and $Pm\bar{3}n$ structures and the atomic *Fddd* structure are metallic, they are attractive candidates for superconductivity, especially considering that both I and Br become superconducting in their atomic phase. Although the T_c of I and Br are below 2 K, F solids might exhibit higher phonon frequency and stronger electron-phonon coupling because of its lower atomic mass and stronger covalent bonds, both factors might improve the T_c. The Eliashberg function, electron-phonon coupling (EPC) constant, and logarithmic average phonon frequency $\omega_{\log}$ are calculated to investigate the superconductivity (see Fig. 5 and Table SI in the Supplemental Material [25]). For $P6/mcc$ structure, the EPC calculation yields a small λ of 0.29 and a large $\omega_{\log}$ of 1382 K at 3 TPa. In the cases of the $Pm\bar{3}n$ and *Fddd* phases, the calculated λ is 0.38 and 0.44, and $\omega_{\log}$ is 1923 and 2224 K at 5 and 30 TPa, respectively. The T_c for the three phases are calculated using the Allen-Dynes-modified McMillan equation [35]

$$T_c = \frac{\omega_{\log}}{1.2}\exp\left[\frac{1.04(1+\lambda)}{\lambda - \mu^*(1+0.62\lambda)}\right],$$

where μ^* is the Coloumb pseudopotential, with typical values of 0.10 and 0.13. The calculated T_c is low, at 0.3–1.3 K, for the $P6/mcc$ structure at 3 TPa, 2.1–5.5 K for the $Pm\bar{3}n$ structure at 5 TPa, and 8.4–16.1 K for *Fddd* at 30 TPa. The predicted T_c for the atomic phase is larger than that of the two intermediate phases, which is due to the large λ and $\omega_{\log}$.

Finally, we discuss the cause of this unconventional multistep structural evolution toward the complete dissociation of the F—F bonds and the transformation of solid F to the atomic phase. First, the internal energy U and the pV, the two terms of enthalpy, are shown separately as functions of pressure for the four stable structures (see Fig. S6 in the Supplemental Material [25]). It reveals that the major driving force for the structure evolution under pressure is the volume reduction. The results reveal very different trends for pV and U under pressure. Under an increasing pressure of up to 5 TPa, the intermediate structures show an advantage due to the reduced volume relative to the *Cmca* structure. Their internal energies are higher than that of the *Cmca* structure, but the differences dwindle. It is the combination of U and pV that stabilizes these intermediate phases. Between the two intermediate phases, Pm-$3n$ has the smaller volume at both low and high

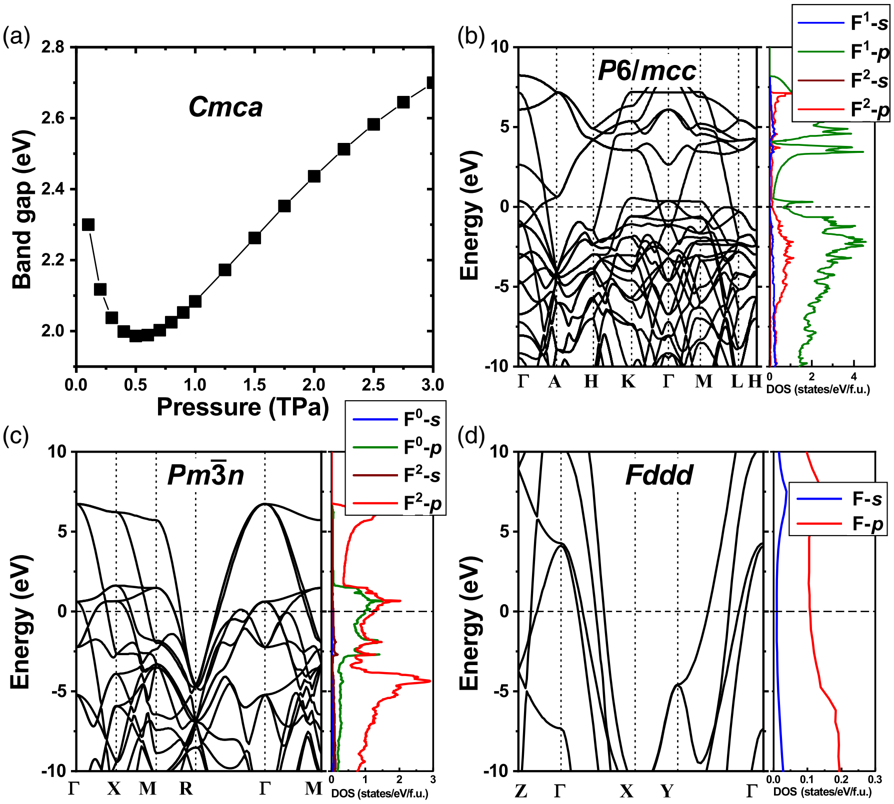

FIG. 4. (a) Variation of band gaps with pressure for $Cmca$. Band structure and partial densities of states (PDOSs) of (b) $P6/mcc$ phase at 3 TPa, (c) $Pm\bar{3}n$ phase at 5 TPa, and (d) $Fddd$ at 30 TPa.

pressures. Its internal energy is higher but becomes smaller than $P6/mcc$ at 27 TPa. Comparing these structures, we find that the atomic phase $Fddd$ shows a higher internal energy throughout the pressure range. However, its volume and therefore its pV reduces rapidly with increasing pressure. The pV term becomes lower than $P6/mcc$ at 6 TPa and lower than Pm-3n at 8 TPa. However, only at 30 TPa, when the reduction in pV overcomes the large excess U, does $Fddd$ become the most stable structure. Therefore, the transformation of F to the atomic phase is mainly driven by the volume reduction under pressure. This is in marked difference to H, in which the atomic phase is caused by both the volume reduction and the change of the electronic structure.

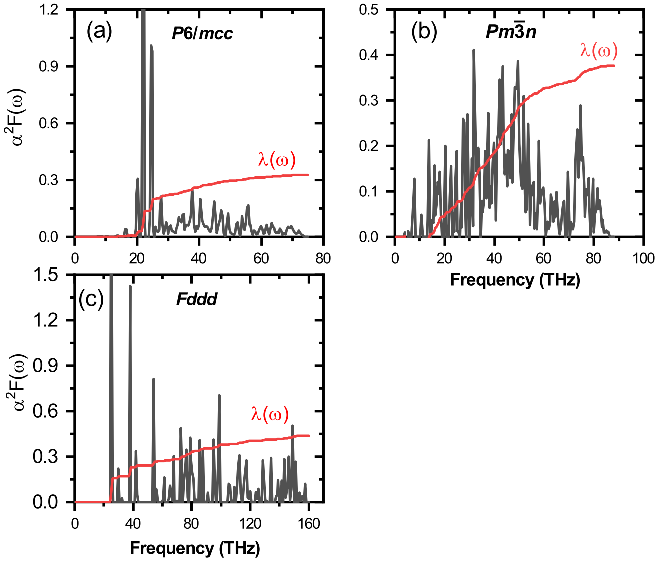

FIG. 5. The calculated Eliashberg function $\alpha^2F(\omega)$ (black lines) and EPC coefficient λ (red lines) of (a) $P6/mcc$ at 3 TPa, (b) $Pm\bar{3}n$ at 5 TPa, and (c) $Fddd$ at 30 TPa.

The intricate structural evolution of F and the general trend of pV and U under pressure is due largely to the competition between the reduced volume and the lone pair electrons of F that, compared to all other elements, is the hardest to compress. Although the atomic phase has the smallest volume that favors its formation under pressure, the complete quench of the lone pairs in this structure greatly increases its internal energy. In the pressure range 2.8–30 TPa, F solid compromises the volume reduction and the quench of the lone pairs by adopting the two intermediate structures. In these structures, the lone pairs are only partially quenched because the open interstitial spaces leave room for lone pairs, although they are compelled to deform and rehybridize in these structures. The reduced volume eventually overcomes the large internal energy increase of the atomic structure caused by the quench of the lone pairs, however, the required pressure is much higher than it is for other elements, including H and O.

In summary, using a crystal structure prediction method based on DFT calculations, we have thoroughly studied the structural evolution of solid F under high pressure and found a unique multistep transformation from low-pressure molecular structures to an atomic phase which has not been seen in any other elementary solid. Compared to H, N, O, and other halogens, F is extremely resistant to becoming an atomic phase and reaches that destination of all elements only under an exceedingly high pressure of 30 TPa. Most strikingly, the structural evolution undergoes two intermediate steps with high-symmetry structures, $P6/mcc$ and $Pm\bar{3}n$, that contain the mixture of F_2 molecules and F line chains and the mixture of F line chains and F atoms, respectively. Both the intermediate structures and the eventual atomic phase with $Fddd$ symmetry are metallic and become superconducting, although the T_c are only at the level of 1 to a few kelvins.

This work was supported by the National Key R&D Program of China (Grant No. 2018YFA0305900) and the National Natural Science Foundation of China (Grants No. 11674122, No 51632002, and No. 52072188). C. J. P. acknowledges financial support from the Engineering and Physical Sciences Research Council (Grant No. EP/P022596/1]. M. M. acknowledges the support of the NSF CAREER fund (Grant No. 1848141) and the ACS PRF fund (Grant No. 59249-UNI6). Some of the calculations were performed at the High Performance Computing Center (HPCC) of Jilin University and using TianHe-1(A) at the National Supercomputer Center in Tianjin.

---

[*] Corresponding authors.
cuitian@nbu.edu.cn; cuitian@jlu.edu.cn
mmiao@csun.edu

[1] J. M. McMahon and D. M. Ceperley, Ground-State Structures of Atomic Metallic Hydrogen, Phys. Rev. Lett. **106**, 165302 (2011).

[2] C. J. Pickard and R. J. Needs, Structure of phase III of solid hydrogen, Nat. Phys. **3**, 473 (2007).

[3] C. J. Pickard, M. Martinez-Canales, and R. J. Needs, Density functional theory study of phase IV of solid hydrogen, Phys. Rev. B **85**, 214114 (2012).

[4] R. T. Howie, C. L. Guillaume, T. Scheler, A. F. Goncharov, and E. Gregoryanz, Mixed Molecular and Atomic Phase of Dense Hydrogen, Phys. Rev. Lett. **108**, 125501 (2012).

[5] A. F. Goncharov, E. Gregoryanz, H.-k. Mao, Z. Liu, and R. J. Hemley, Optical Evidence for a Nonmolecular Phase of Nitrogen above 150 GPa, Phys. Rev. Lett. **85**, 1262 (2000).

[6] M. I. Eremets, R. J. Hemley, H.-k. Mao, and E. Gregoryanz, Semiconducting non-molecular nitrogen up to 240 GPa and its low-pressure stability, Nature (London) **411**, 170 (2001).

[7] X. Wang *et al.*, Cagelike Diamondoid Nitrogen at High Pressures, Phys. Rev. Lett. **109**, 175502 (2012).

[8] J. Sun, M. Martinez-Canales, D. D. Klug, C. J. Pickard, and R. J. Needs, Stable All-Nitrogen Metallic Salt at Terapascal Pressures, Phys. Rev. Lett. **111**, 175502 (2013).

[9] L. Zhu, Z. Wang, Y. Wang, G. Zou, H.-k. Mao, and Y. Ma, Spiral chain O_4 form of dense oxygen, Proc. Natl. Acad. Sci. U.S.A. **109**, 751 (2012).

[10] J. Sun, M. Martinez-Canales, D. D. Klug, C. J. Pickard, and R. J. Needs, Persistence and Eventual Demise of Oxygen Molecules at Terapascal Pressures, Phys. Rev. Lett. **108**, 045503 (2012).

[11] L. Meyer, C. S. Barrett, and S. C. Greer, Crystal structure of α-fluorine, J. Chem. Phys. **49**, 1902 (1968).

[12] Q. Lv, X. Jin, T. Cui, Q. Zhuang, Y. Li, Y. Wang, K. Bao, and X. Meng, Crystal structures and electronic properties of solid fluorine under high pressure, Chin. Phys. B **26**, 076103 (2017).

[13] Q. Zeng, Z. He, X. San, Y. Ma, F. Tian, T. Cui, B. Liu, G. Zou, and H. k. Mao, A new phase of solid iodine with different molecular covalent bonds, Proc. Natl. Acad. Sci. U.S.A. **105**, 4999 (2008).

[14] T. Kenichi, S. Kyoko, F. Hiroshi, and O. Mitsuko, Modulated structure of solid iodine during its molecular dissociation under high pressure, Nature (London) **423**, 971 (2003).

[15] Y. Fujii, K. Hase, N. Hamaya, Y. Ohishi, A. Onodera, O. Shimomura, and K. Takemura, Pressure-Induced Face-Centered-Cubic Phase of Monatomic Metallic Iodine, Phys. Rev. Lett. **58**, 796 (1987).

[16] D. Duan, Y. Liu, Y. Ma, Z. Liu, T. Cui, B. Liu, and G. Zou, Ab initio studies of solid bromine under high pressure, Phys. Rev. B **76**, 104113 (2007).

[17] P. Li, G. Gao, and Y. Ma, Modulated structure and molecular dissociation of solid chlorine at high pressures, J. Chem. Phys. **137**, 064502 (2012).

[18] P. Dalladay-Simpson, J. Binns, M. Peña-Alvarez, M.-E. Donnelly, E. Greenberg, V. Prakapenka, X.-J. Chen, E. Gregoryanz, and R. T. Howie, Band gap closure, incommensurability and molecular dissociation of dense chlorine, Nat. Commun. **10**, 1134 (2019).

[19] K. Shimizu, K. Amaya, and N. Suzuki, Pressure-induced superconductivity in elemental materials, J. Phys. Soc. Jpn. **74**, 1345 (2005).

[20] D. Duan, X. Jin, Y. Ma, T. Cui, B. Liu, and G. Zou, Effect of nonhydrostatic pressure on superconductivity of monatomic iodine: An ab initio study, Phys. Rev. B **79**, 064518 (2009).

[21] D. Duan *et al.*, The crystal structure and superconducting properties of monatomic bromine, J. Phys. Condens. Matter **22**, 015702 (2010).

[22] A. R. Oganov, C. J. Pickard, Q. Zhu, and R. J. Needs, Structure prediction drives materials discovery, Nat. Rev. Mater. **4**, 331 (2019).

[23] C. J. Pickard and R. J. Needs, High-Pressure Phases of Silane, Phys. Rev. Lett. **97**, 045504 (2006).

[24] C. J. Pickard and R. J. Needs, Ab initio random structure searching, J. Phys. Condens. Matter **23**, 053201 (2011).

[25] See Supplemental Material at http://link.aps.org/supplemental/10.1103/PhysRevLett.126.225704, which includes Refs. [23,24,26–31], for computational details, the

functionals and pseudopotentials test, phonon dispersion curves, pV and internal energy U with pressure, the calculated T_c, and structural information for all of the predicted structures.

[26] M. D. Segall, J. D. L. Philip, M. J. Probert, C. J. Pickard, P. J. Hasnip, S. J. Clark, and M. C. Payne, First-principles simulation: ideas, illustrations and the CASTEP code, J. Phys. Condens. Matter **14**, 2717 (2002).

[27] J. P. Perdew, K. Burke, and M. Ernzerhof, Generalized Gradient Approximation Made Simple, Phys. Rev. Lett. **77**, 3865 (1996).

[28] G. Kresse and J. Furthmüller, Efficient iterative schemes for ab initio total-energy calculations using a plane-wave basis set, Phys. Rev. B **54**, 11169 (1996).

[29] A. Togo, F. Oba, and I. Tanaka, First-principles calculations of the ferroelastic transition between rutile-type and $CaCl_2$-type SiO_2 at high pressures, Phys. Rev. B **78**, 134106 (2008).

[30] G. Paolo *et al.*, Quantum ESPRESSO: A modular and open-source software project for quantum simulations of materials, J. Phys. Condens. Matter **21**, 395502 (2009).

[31] P. Blaha, K. Schwarz, P. Sorantin, and S. Trickey, Full-potential, linearized augmented plane wave programs for crystalline systems, Comput. Phys. Commun. **59**, 399 (1990).

[32] D. Melicherová, O. Kohulák, D. Plašienka, and R. Martoňák, Structural evolution of amorphous polymeric nitrogen from ab initio molecular dynamics simulations and evolutionary search, Phys. Rev. Mater. **2**, 103601 (2018).

[33] H. Zhang *et al.*, Pressure-induced amorphization and existence of molecular and polymeric amorphous forms in dense SO_2, Proc. Natl. Acad. Sci. U.S.A. **117**, 8736 (2020).

[34] A. V. Krukau, O. A. Vydrov, A. F. Izmaylov, and G. E. Scuseria, Influence of the exchange screening parameter on the performance of screened hybrid functionals, J. Chem. Phys. **125**, 224106 (2006).

[35] P. B. Allen and R. C. Dynes, Transition temperature of strong-coupled superconductors reanalyzed, Phys. Rev. B **12**, 905 (1975).

Correction: The footnote indicator for “Corresponding author” was missing for the eighth author and has been inserted.